ORIGINAL PAPER

Phase diagram of Au-Al-Cu at 500 °C

Jyun Lin Li · Pei Jen Lo · Ming Chi Ho ·
Ker-Chang Hsieh

Abstract Diffusion couples and equilibrated alloys were used to construct the isothermal phase diagram of Au-Al-Cu at 500 °C. Electron microprobe analyses were performed to determine the phase compositions and phase relationships. Two ternary phases and 10 three-phase equilibriums were determined in this study. Four additional three-phase equilibriums were estimated to meet the criteria for phase relationships. The δ (Au₂Al) phase exhibited a wide range of solubility, and the lattice parameters were examined by X-ray. The solubility ranges of the binary intermetallic phases were also determined.

Keywords Phase diagram · Au-Al-Cu · Au-base alloy · Phase diagram · Diffusion couple

Introduction

Gold wire has been used as bonding wire in IC packages because of its ductility and anticorrosion characteristics. Recently, the increase in the I/O number of ICs from 200 to 300 has required diameter of gold wires to decrease from 25 μm to less than 20 μm to match the decrease in the area of the Al pad. Nevertheless, the stiffness of gold wire must be enhanced to avoid short circuits derived from wire sweep. Au-Cu alloy wire is one of the new alloy bonding wires that has been developed. The bonding wire reacts with the Al pad and forms intermetallic phases to maintain the electrical connection. A low-temperature Au-Al-Cu phase diagram could provide essential information to understand the reactions between the Au-Cu alloy wire and the Al pad. The stability of intermetallic phases is closely related to the reliability of wire bonding [1, 2].

A β (Au₇Al₄Cu₅) phase exhibiting martensite-like properties was developed [3–5]. The embossed and fine-layered surface of this material, which originates from a martensitic transformation, exhibits a characteristic shining color and is used in Spangold jewelry.

Binary systems in Au-Al-Cu systems have been studied in depth. Al-Au binary systems exhibit five intermediate phases at 500 °C, namely, AuAl₂, AuAl, Au₂Al, Au₈Al₃ (Au₅Al₂), and Au₄Al [6]. Al-Cu binary systems exhibit five intermediate phases at 500 °C, namely, θ (Al₂Cu), η₂ (AlCu), ζ₂ (Al₉Cu₁₁), δ (Al₂Cu₃), and γ₁ phases [7]. Au-Cu binary systems form solid solution at 500 °C [8].

In recent decades, several researchers have studied Au-Al-Cu ternary systems. The isothermal sections of Au-Al-Cu at 500 °C were reported by Levey et al. [9–11] and those at 750 °C by Bhatia et al. [12]. Levey et al. [13] also constructed isopleths for the 76 wt.% Au section. These previous phase-diagram studies were conducted by applying traditional bulk alloy equilibrium. Isothermal phase diagrams were constructed by preparing bulk alloys with various compositions and annealing them at a certain high temperature to reach phase equilibrium. This method is not suitable for constructing gold-based low-temperature phase diagrams because it is too expensive to prepare 30 to 50 samples without recovering the Au precious metal, and it would take much time to reach phase equilibrium because of the low temperature used. This study applied the diffusion couple method to construct the Au-Al-Cu ternary 500 °C phase diagram. This method uses little Au and easily attains the local phase equilibrium within 1 day. In this method, the interface and phases on both sides of the interface reach equilibrium, and the relationships among these phases are thereby elucidated. A detailed diffusion couple theory is available in [14].

J. L. Li · P. J. Lo · M. C. Ho · K.-C. Hsieh (✉)
Department of Materials and Optoelectronic Science, National Sun Yat-Sen University, 70, Lien-Hai Road, Kaohsiung 804, Taiwan
e-mail: khsieh@mail.nsysu.edu.tw

Table 1 Summary of phase equilibria in nine diffusion couples

Diffusion couple	Compositions (at.%) (Al/Au_xCu_{100-x})		Phase equilibria							
	Au	Cu								
D1	90	10	Al-$AuAl_2$	$AuAl_2$-$AuAl$	$AuAl$-δ (Au_2Al)	δ (Au_2Al)-α				
D2	80	20	Al-Al_2Cu-$AuAl_2$	$AuAl_2$-$AuAl$	$AuAl$-δ (Au_2Al)	δ (Au_2Al)-β	δ (Au_2Al)-β-α			
D3	70	30	Al-Al_2Cu	Al_2Cu-$AuAl_2$	$AuAl_2$-$AuAl$	$AuAl$-δ (Au_2Al)-γ	γ-β	β-α		
D4	60	40	Al-Al_2Cu	Al_2Cu-ε-$AlCu$	$AlCu$-$AuAl_2$	$AuAl_2$-γ	γ-β	β-α		
D5	50	50	Al-Al_2Cu	Al_2Cu-ε-$AlCu$	$AlCu$-Al_9Cu_{11}	Al_9Cu_{11}-Al_2Cu_3	Al_2Cu_3-$AuAl_2$	$AuAl_2$-γ	γ-β	β-α
D6	40	60	Al-Al_2Cu	Al_2Cu-ε-$AlCu$	$AlCu$-$AuAl_2$-Al_9Cu_{11}	Al_9Cu_{11}-Al_2Cu_3	Al_2Cu_3-$AuAl_2$	$AuAl_2$-γ	γ-β	β-α
D7	30	70	Al-Al_2Cu	Al_2Cu-ε-$AlCu$	$AlCu$-$AuAl_2$-Al_9Cu_{11}	Al_2Cu_3-$AuAl_2$	$AuAl_2$-γ	γ-β	β-α	
D8	20	80	Al-Al_2Cu	Al_2Cu-ε-$AlCu$	$AlCu$-Al_9Cu_{11}-$AuAl_2$	Al_9Cu_{11}-Al_2Cu_3-$AuAl_2$	Al_2Cu_3-$AuAl_2$-γ	γ-α		
D9	10	90	Al-Al_2Cu	Al_2Cu-ε-$AlCu$	$AlCu$-Al_9Cu_{11}-$AuAl_2$	Al_9Cu_{11}-Al_2Cu_3-$AuAl_2$	Al_2Cu_3-$AuAl_2$-γ	γ-α		

Experimental procedures

The alloys were prepared through mini arc melting of pure Au, Cu, and Al under a pure Ar atmosphere. Afterward, the samples were cast into a 2-mm diameter ingot bar. Nine Au-Cu binary alloys (D1–D9) and 12 Au-Al-Cu ternary alloys (A1–A12) were prepared for this phase diagram study. The alloy compositions are listed in Tables 1 and 2.

Figure 1 is the schematic diagram of the diffusion couple setup. The Au-Cu binary alloy ingots (D1–D9) were sliced into 1-mm-thick discs, and a pure aluminum bar with a 2-mm diameter was sliced into 2-mm-thick discs. The discs were joined to form a diffusion couple. The screw of the holder exerted pressure on the diffusion couple. The holder was sealed in a quartz tube to form a vacuum, maintained at 500 °C for 24 h, and then quenched in ice water. The ternary alloys (A1–A12) were sealed in the quartz tube vacuum. These alloy samples were maintained at 500 °C for 14–29 days.

An electron probe microanalyzer (EPMA) was used to determine the equilibrium phase compositions of the diffusion couple samples and ternary alloy samples. The isothermal phase diagram of the Au-Al-Cu annealed at 500 °C was constructed based on these results.

Results

The phase equilibria of the diffusion couples are summarized in Table 1. As shown in Figs. 2a, b, the D1 diffusion couple formed the equilibrium phase layers $Al/AuAl_2/AuAl/\delta$ (Au_2Al)/α (Au, Cu). The phase layer thickness of $AuAl_2$ and $AuAl$ was approximately 10 μm each, and the δ (Au_2Al) phase was approximately 300 μm thick. The latter binary phase extends into ternary with large composition range in Cu and Au. The original interface was present within the δ (Au_2Al) phase (Fig. 2a), indicating that the diffusion rates of Cu and Au were faster than that of Al. As shown in Figs. 3a, b, c, the D5 diffusion couple comprised several phase layers: $Al/Al_2Cu/AlCu$ and $\varepsilon/Al_9Cu_{11}/Al_2Cu_3/AuAl_2/\gamma/\beta/\alpha$ (Au, Cu). The line-scan imaging results of the D5 diffusion sample are shown in Fig. 3d. A two-phase layer ($AlCu+\varepsilon$) was in contact with the Al_2Cu phase layer; therefore, the Al_2Cu-ε-$AlCu$ three-phase equilibrium was generated. The existence of this three-phase equilibrium was confirmed through the alloy sample A1 and the equilibrium microstructure (Fig. 4). The phase equilibria of the alloy equilibrium samples are summarized in Table 2. According to the results in Tables 1 and 2, the determined phase diagram is shown in Fig. 5. In the diffusion couple experiment, seven sets of three-phase equilibria, namely, Al-$AuAl_2$-Al_2Cu, Al_2Cu-ε-$AlCu$, γ-$AuAl_2$-Al_2Cu_3, $AuAl$-δ (Au_2Al) -γ, δ (Au_2Al)-α-β, $AlCu$-$AuAl_2$-Al_9Cu_{11}, and Al_9Cu_{11}-$AuAl_2$-Al_2Cu_3 were determined from the phase
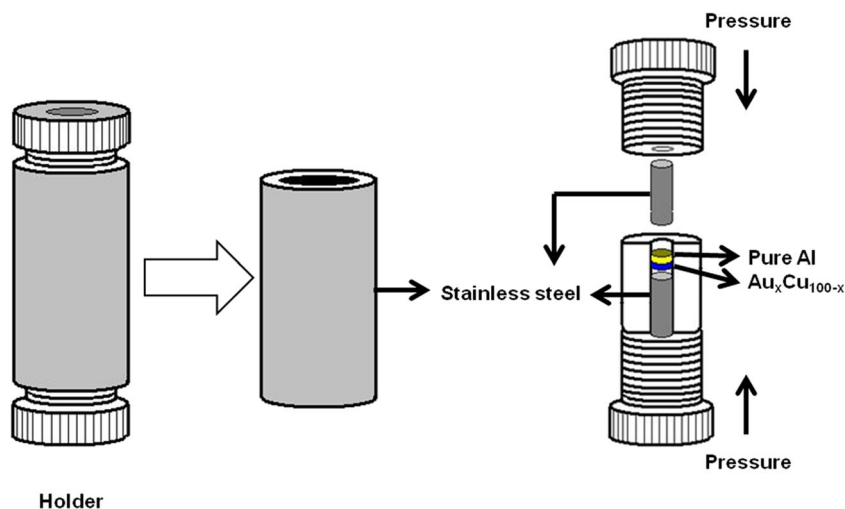
relationships, resembling the result of the Al_2Cu-ε-AlCu three-phase equilibrium shown in Fig. 3c. The other three-
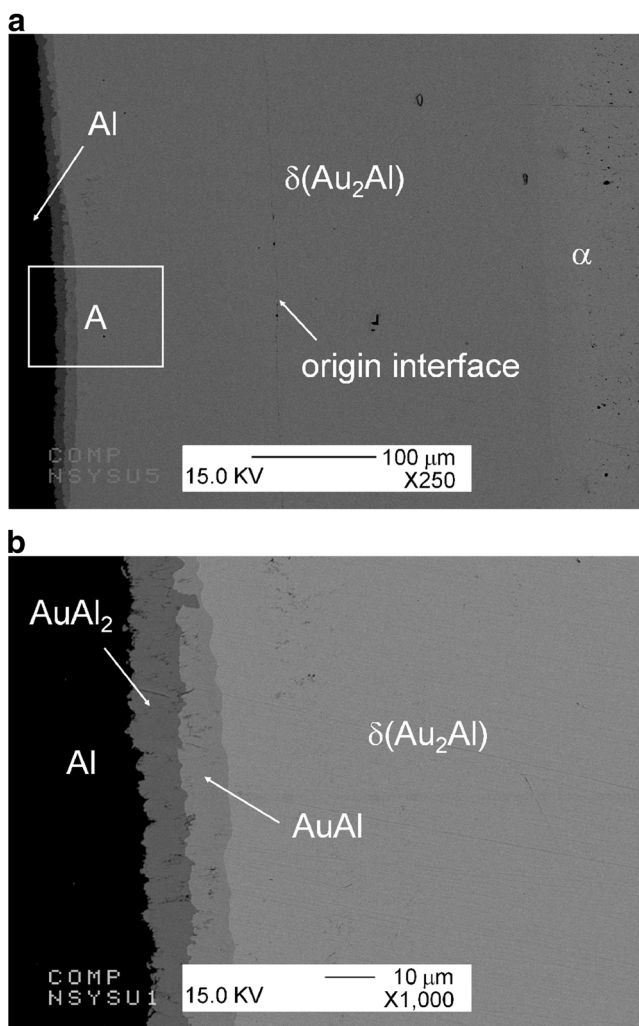

Fig. 2 a The whole view of D1 sample microstructure. **b** The detail phase layers of the A region in (**a**)
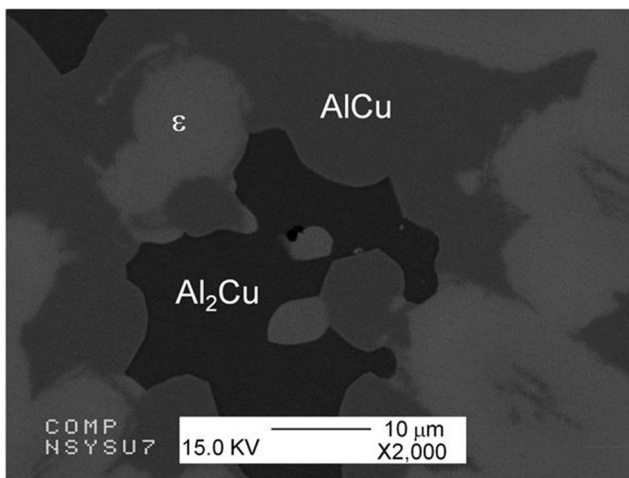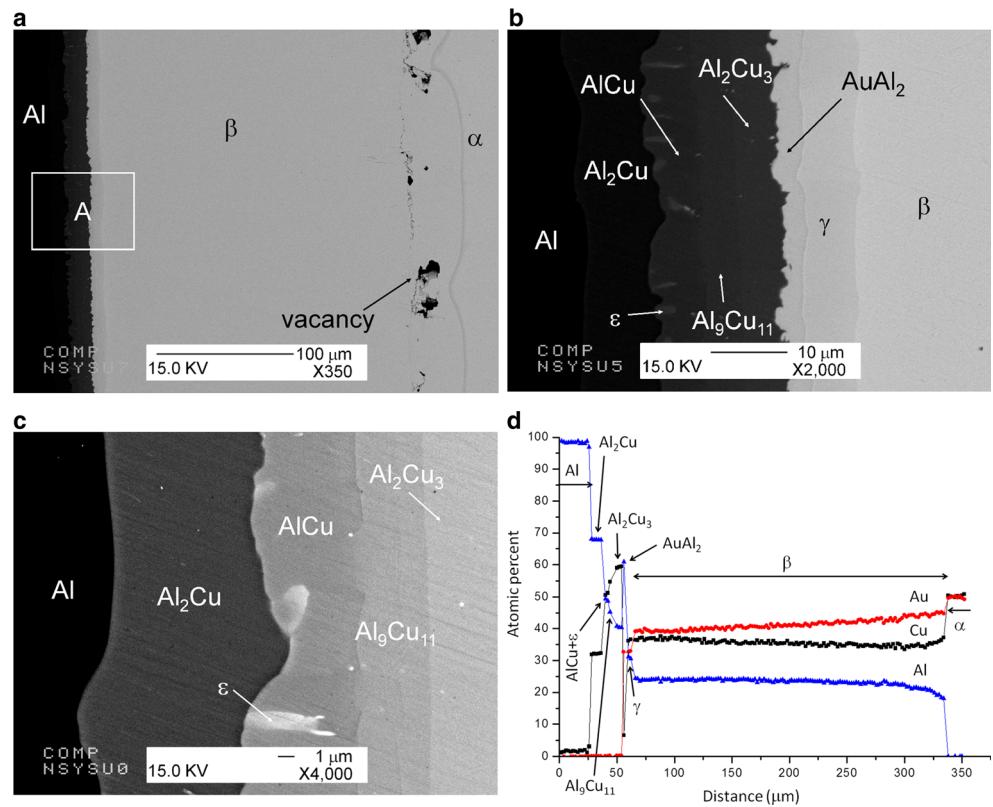
phase equilibria ($AuAl_2$-ε-AlCu, γ-$AuAl_2$-AuAl, and Au_8Al_3-δ (Au_2Al)-Au_4Al) were determined by applying the alloy equilibrium methods to alloy samples A2, A3, and A5 (Table 2). These 10 sets of three-phase equilibria are shown as solid lines in Fig. 5. In addition, the $AuAl_2$-ε-Al_2Cu three-phase equilibria were determined based on their two-phase equilibria. The other three sets of three-phase equilibria were estimated to meet the phase relationships shown as dashed lines in Fig. 5. The diffusion paths of D1 and D5 are plotted in Fig. 6, covering most of the binary and ternary phases. All of the binary intermediate phases in Al-Au [6] and Al-Cu [7] were identified in this study. For the Au-Cu [8] system, only the α (Au, Cu) phase appeared at 500 °C. The solubility of Al in the α (Au, Cu) phase was determined using an EPMA.

Figure 7 shows the Au-Al-Cu isothermal section obtained through bulk alloy equilibrium at 500 °C, reported by Levey et al. [9–11]. According to this study, the maximum Au solubility in the γ-$AlCu_2$ phase reached 48 at.%, agreeing with the result of Levey et al. [9–11]. The composition range and shape of the ternary β phase reported by these authors was confirmed in this study. In the D3–D7 samples, the β phase layer was present between the γ phase and α phase layers.

Ternary phase δ (Au_2Al) was also identified in this study. The homogeneity range of the δ (Au_2Al) phase was primarily determined from the composition range of the single-phase diffusion layer in the D1, D2, and D3 diffusion couples. The line-scan imaging results of the D1 diffusion sample are shown in Fig. 8. The peculiar concave shape was confirmed by analyzing the A4, A8, and A9 alloy samples, and the microstructure and compositions of tie lines between the δ (Au_2Al) and β phases are shown in Fig. 9. The crystal structure of δ (Au_2Al) phase was examined by X-ray in the A4, A8, A11, and A12 alloy samples. The lattice parameters are plotted and listed in Fig. 10.

The ε ternary phase identified in the D4–D9 diffusion couples comprised with AlCu phase as two-phase layer in

Fig. 3 a The whole view of D5 sample microstructure. b The detail phase layers of the A region in (a) as Al/Al$_2$Cu/AlCu, ε/Al$_9$Cu$_{11}$/Al$_2$Cu$_3$/AuAl$_2$/γ/β. c The detail phase layers of the A region in (a) as Al/Al$_2$Cu/AlCu, ε/Al$_9$Cu$_{11}$/Al$_2$Cu$_3$. d A composition profile of the D5 sample measured by EPMA

equilibrium with an AuAl$_2$ phase layer (Fig. 3c). The ε phase was not present as a single-phase layer in these diffusion couples. The composition range was determined using the three-phase equilibria of the Al$_2$Cu-ε-AlCu and AuAl$_2$-ε-

Fig. 4 The microstructure of A1 alloy sample including Al$_2$Cu, ε and AlCu phases

Color	Phase	Composition (at.%)		
		Au	Cu	Al
light gray	ε	4.21±0.30	33.39±0.57	62.40±0.58
dark gray	AlCu	none	49.48±1.12	50.49±0.13
black	Al$_2$Cu	none	32.31±1.81	67.67±1.81

Table 2 Summary of phase equilibria in 12 bulk alloy samples

Alloy	Alloy compositions (at.%) (Au$_x$Cu$_y$Al$_{100-x-y}$)			Phase equilibria
	Au	Cu	Al	
A1	2	39	59	Al$_2$Cu-ε-AlCu
A2	18	17	65	AuAl$_2$-ε-AlCu
A3	40	6	54	AuAl$_2$-AuAl-γ
A4	57.5	10	32.5	δ (Au$_2$Al)-β
A5	72	6	22	Au$_8$Al$_3$-δ (Au$_2$Al)-Au$_4$Al
A6	45	40	15	β-α
A7	47	39	14	β-α
A8	58	14	28	δ (Au$_2$Al)-β
A9	62	13	25	δ (Au$_2$Al)-β
A10	68	6	26	Au$_8$Al$_3$-δ (Au$_2$Al)
A11	68	11	21	δ (Au$_2$Al)
A12	62	6	32	δ (Au$_2$Al)

AlCu of the A1 and A2 alloy samples, respectively. The equilibrium microstructure and microprobe analysis results are shown in Figs. 4 and 11. The ε phase contained 25 to 33.4 at.% of Cu and 62.4 to 65 at.% of Al.

Discussion

In this study, a classical semi-infinite diffusion couple was applied, meaning that the end couples maintained their

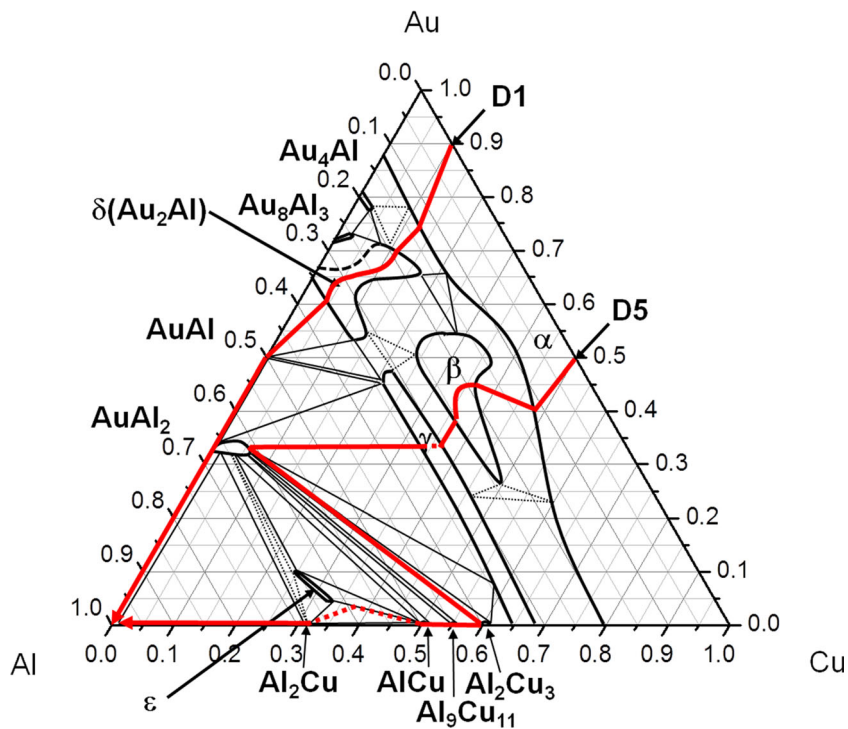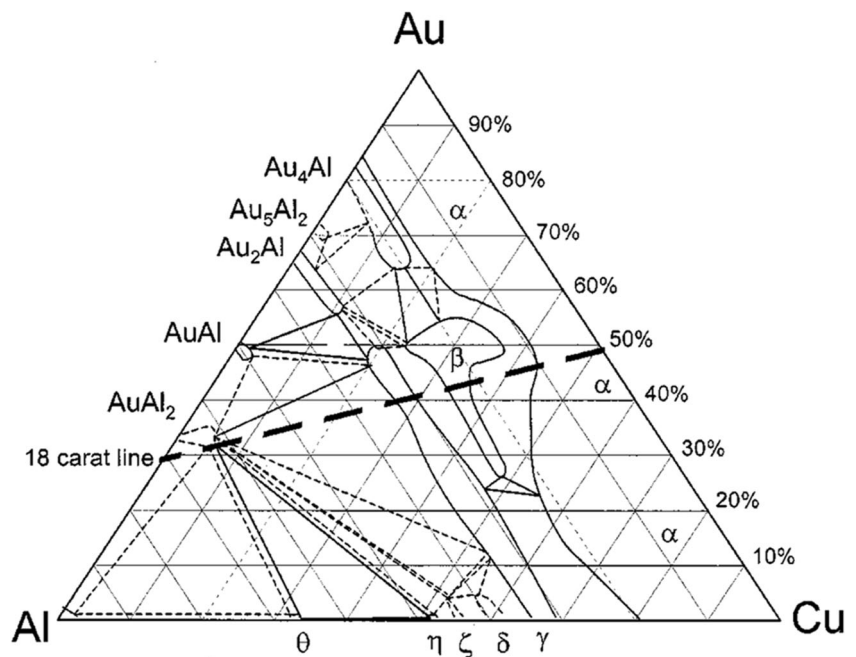**Fig. 6** The diffusion paths of D1 and D5 samples

original compositions after the diffusion couple annealing. If
volume diffusion in a semi-infinite couple is a rate-limiting
step, local equilibrium is assumed to exist, in which case the
rules described previously can be used to relate the reaction
zone morphology developed during isothermal diffusion to
the phase diagram. The phase composition of the reaction
zone is independent of time, whereas that of the diffusion path
is fixed. A D8 diffusion couple was annealed for 5 days to
compare it with the 1-day diffusion couple. No difference was
observed among the phases formed in each diffusion layer,
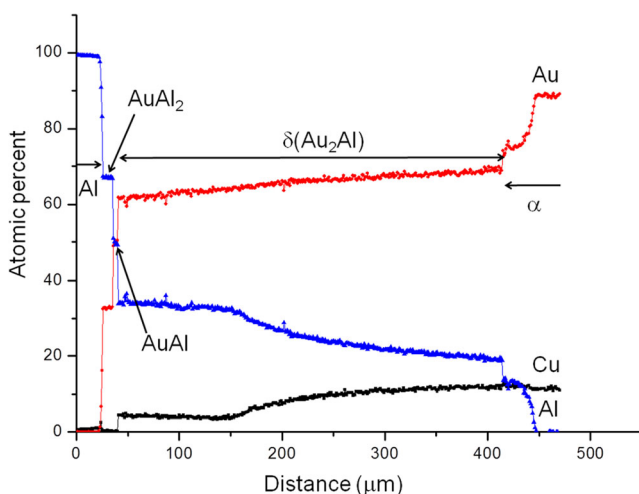
Fig. 8 A composition profile of the D1 sample measured by EPMA

and only the layer thickness differed. The versatility of
this technique for constructing isothermal cross sections
of ternary systems has been demonstrated repeatedly
[14].

The D2 diffusion path was plotted on the Au-rich region
(Fig. 12a), and its corresponding microstructure is shown in
Figs. 12b, c. The solid a-b line crossed the α single-phase field,
and the dashed b-c line crossed the δ (Au$_2$Al)-α-β three-phase
region, indicating the presence of an interface in the diffusion
structure, with equilibrium between the α single-phase and δ
(Au$_2$Al)-β two-phase region. The microstructure of the corre-
sponding three-phase region is shown in Fig. 12b and is marked
as the interface b-c; c-d is the δ (Au$_2$Al)-β two-phase region. The
solid d-e-f-g line in Fig. 12a shows that the diffusion path entered
the δ (Au$_2$Al) single-phase region, returned to the δ (Au$_2$Al)-β
two-phase region, and then entered the δ (Au$_2$Al) single-phase
region again. The thickness of the δ (Au$_2$Al)-β two-phase region
was approximately 150 µm and was contained within the δ
(Au$_2$Al) single-phase region. Figure 12c shows the other side
of this microstructure. This diffusion path could explain why the
β phase formed within the δ (Au$_2$Al) phase layer.

The diffusion paths D8 and D9 crossed three three-phase
regions (AlCu-AuAl$_2$-Al$_9$Cu$_{11}$, Al$_9$Cu$_{11}$-AuAl$_2$-Al$_2$Cu$_3$, and
γ-AuAl$_2$-Al$_2$Cu$_3$) with AuAl$_2$ as the common matrix phase.
Figure 13a shows the diffusion path near the Al-Cu binary
region, and Fig. 13b is the plot displaying the equilibrium of
these three phases along with their related two-phase regions.
According to Fig. 13b, d-e is the γ-AuAl$_2$-Al$_2$Cu$_3$ three-phase

Fig. 9 The microstructure and tie lines of δ (Au₂Al) and β phases determined from A4, A8, and A9 alloy samples
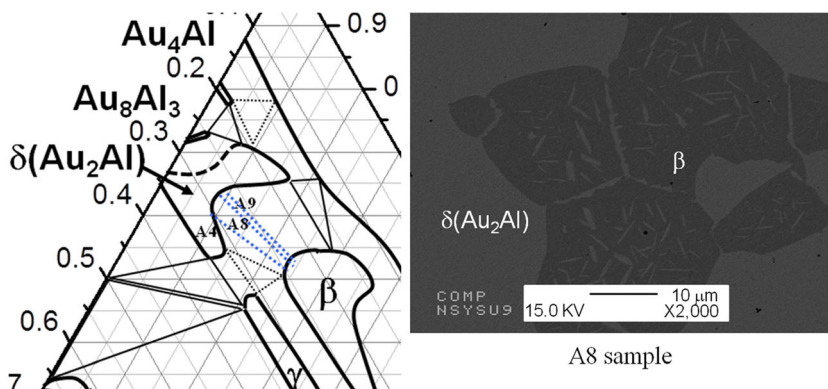
Sample	Phase	Composition (at.%)		
		Au	Cu	Al
A4	δ(Au₂Al)	60.22±0.25	9.21±0.28	30.57±0.19
	β	51.52±0.46	23.70±0.55	24.78±0.97
A8	δ(Au₂Al)	62.86±0.70	9.04±0.34	28.10±0.39
	β	51.46±1.15	24.69±0.79	23.86±0.89
A9	δ(Au₂Al)	62.71±0.89	10.29±0.38	27.00±0.69
	β	52.49±0.34	24.32±0.48	23.19±0.36

equilibrium, e-f is the $AuAl_2$-Al_2Cu_3 two-phase region, f-g is the Al_9Cu_{11}-$AuAl_2$-Al_2Cu_3 three-phase equilibrium, g-h is the Al_9Cu_{11}-$AuAl_2$ two-phase region, h-i is the AlCu-$AuAl_2$-Al_9Cu_{11} three-phase equilibrium, i-j is AlCu-$AuAl_2$, j-k is the AlCu single-phase region, k-l is the ε-AlCu two-phase region, and l-m is the ε-AlCu-Al_2Cu three-phase equilibrium.
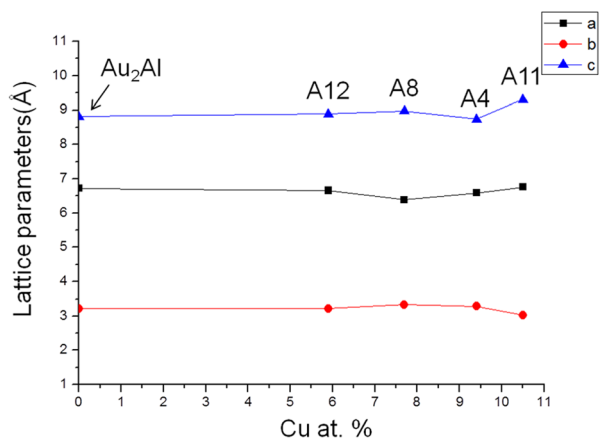
Sample	Phase	Lattice parameters(Å)		
		a	b	c
JC-PDF(65-1504)	Au₂Al	6.715	3.219	8.815
A12	δ(Au₂Al)	6.66±0.01	3.22±0.00	8.89±0.01
A8	δ(Au₂Al)	6.39±0.02	3.33±0.01	8.98±0.01
A4	δ(Au₂Al)	6.59±0.01	3.28±0.00	8.74±0.00
A11	δ(Au₂Al)	6.76±0.02	3.03±0.01	9.31±0.00

Fig. 10 The lattice parameters of δ (Au₂Al) phase
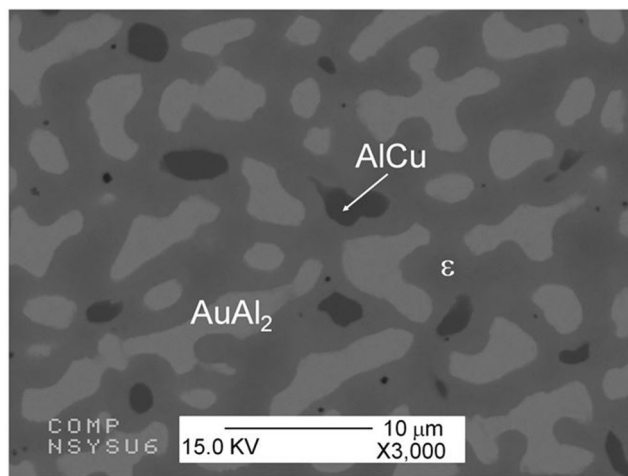
Color	Phase	Composition (at.%)		
		Au	Cu	Al
light gray	AuAl₂	31.30±0.82	4.27±0.37	64.42±0.64
dark gray	ε	15.24±1.03	20.46±1.22	64.30±0.42
black	AlCu	1.867±0.87	46.60±1.61	51.53±0.82

Fig. 11 The microstructure of A2 alloy sample including AuAl₂, ε and AlCu phases
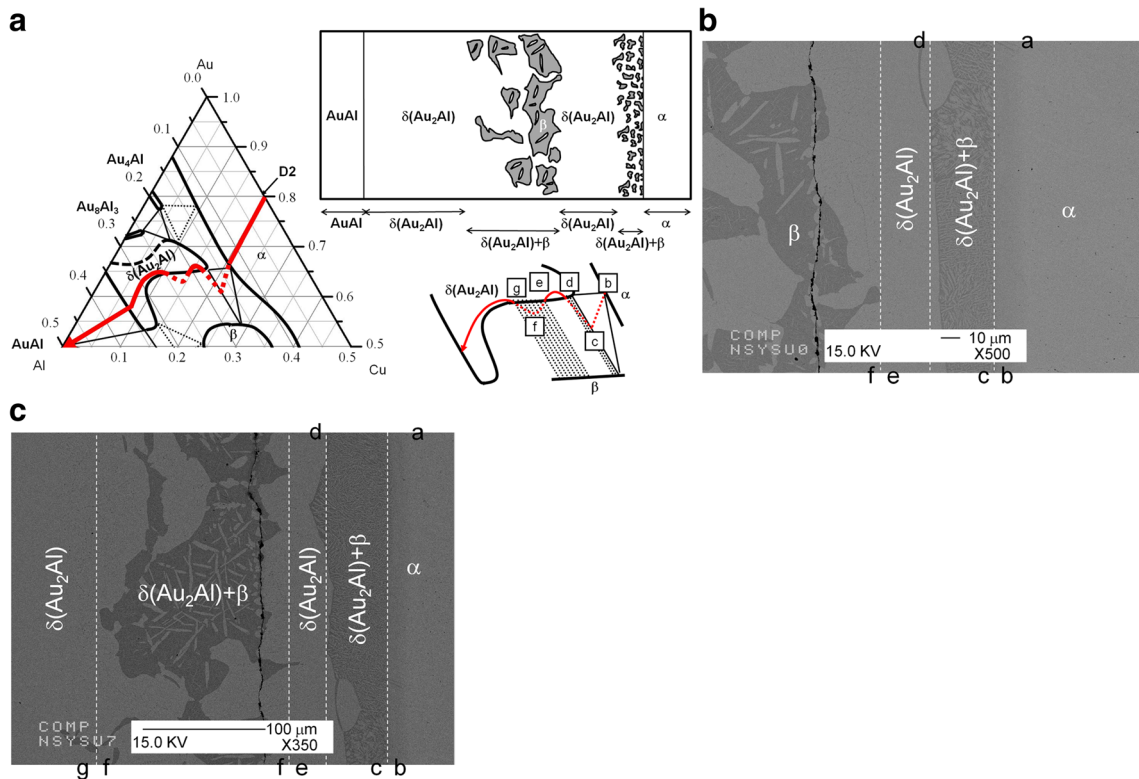
Fig. 12 **a** The diffusion path of D2 diffusion couple and sketch figure. **b** The microstructure of D2 diffusion couple with the label (*a* to *f*) **c** The microstructure of D2 diffusion couple shows β phase formed within δ (Au₂Al) phase with the label (*e* to *g*)
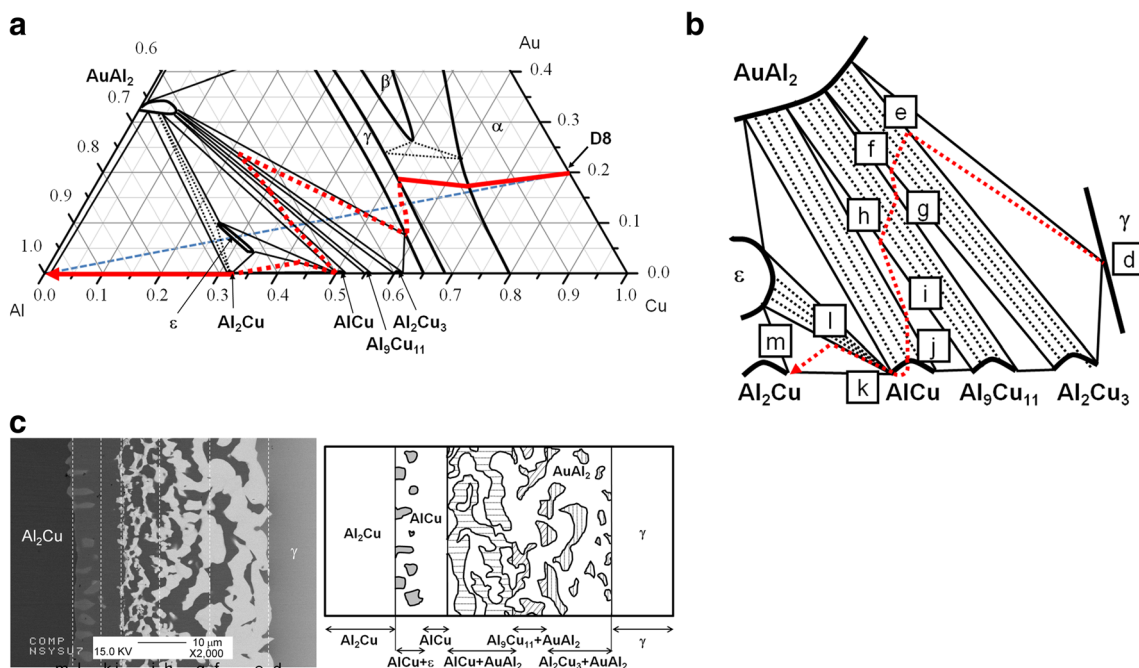

Fig. 13 **a** The diffusion path of D8 diffusion couple near the Al-Cu binary region. **b** The sketch figure of D8 diffusion path. **c** The microstructure of D8 diffusion couple with the label (*d* to *m*) and sketch figure

The microstructure and corresponding sketch are shown in Fig. 13c, and are labeled from d to m, as described previously.

In comparison with Levey [9–11], new ternary phase ε and their related three-phase equilibria were identified in this study. Ternary ε phase exhibited a composition similar to that of the binary Al_2Cu phase and contained 25 to 33.4 at.% of Cu and 62.4 to 65 at.% of Al. Three related three-phase equilibria were also observed, namely, $AuAl_2$-ε-$AlCu$, Al_2Cu-ε-$AlCu$, and $AuAl_2$-ε-Al_2Cu. The β phase reported by Levey was also identified. However, the phase relationships exhibited some differences, because the δ (Au_2Al) phase exhibited a wide range of solubility and a peculiarly shaped phase field in the Au-rich region. Therefore, three additional three-phase equilibria (β-δ (Au_2Al)-α, β-α-γ, and β-δ (Au_2Al)-γ) were identified in this study. Finally, the solubility of Au in the Al_9Cu_{11} and Al_2Cu_3 phases was limited.

Conclusion

The isothermal section of an Au-Al-Cu system annealed at 500 °C was presented in this study. The whole composition range included two ternary phases (ε and β) and 14 three-phase equilibria. The δ (Au_2Al) phase exhibited a wide range of solubility and a peculiar morphology. The ε phase contained 25 to 33.4 at.% of Cu and 62.4 to 65 at.% of Al. Ten three-phase equilibria were determined in this study, namely, Al-$AuAl_2$-Al_2Cu, Al_2Cu-ε-$AlCu$, $AuAl_2$-ε-$AlCu$, $AuAl_2$-$AuAl$-γ, $AuAl$-δ (Au_2Al)-γ, δ (Au_2Al)-α-β, Au_8Al_3-δ (Au_2Al)-Au_4Al, $AlCu$-$AuAl_2$-Al_9Cu_{11}, Al_9Cu_{11}-$AuAl_2$-Al_2Cu_3, and Al_2Cu_3-$AuAl_2$-γ. Four three-phase equilibria, namely, β-δ (Au_2Al)-γ, α-β-γ, α-δ (Au_2Al)-Au_4Al, and $AuAl_2$-ε-Al_2Cu were estimated to meet the criteria for phase relationships.

References

1. Chang HS, Hsieh KC, Martens T, Yang A (2003) The effect of Pd and Cu in the intermetallic growth of alloy Au wire. J Electron Mater 32: 1182–1187
2. Gam SA, Kim HJ, Cho JS, Park YJ, Moon JT, Paik KW (2006) Effects of Cu and Pd addition on Au bonding wire/Al pad interfacial reactions and bond reliability. J Electron Mater 35:2048–2055
3. Cortie MB, Levey FC (2000) Structure and ordering of the 18-carat Al-Au-Cu β-phase. Intermetallics 8:793–804
4. Levey FC, Cortie MB (2001) Body-centred tetragonal martensite formed from $Au_7Cu_5Al_4$ β phase. Mater Sci Eng 303:1–10
5. Levey FC, Cortie MB, Cornish LA (2000) Displacive transformations in Au-18 Wt Pct Cu-6 Wt Pct Al. Metall Mater Trans A 31: 1917–1923
6. Okamoto H (1991) Al-Au (aluminum-gold). J Phase Equilib 12:114–115
7. Murray JL (1985) The aluminium-copper system. Int Mater Rev 30: 211–234
8. Okamoto H, Shakrabarti DJ, Laughlin DE, Massalski TB (1987) The Au-Cu (gold-copper) system. Bull Alloy Phase Diagr 8:454–473
9. Levey FC, Cortie MB, Cornish LA (2002) A 500 °C isothermal section for the Al-Au-Cu system. Metall Mater Trans A 33:987–993
10. Raghavan V (2008) Al-Au-Cu (aluminum-gold-copper). J Phase Equilib Diff 29:260–261
11. Bhatia VK, Levey FC, Kealley CS, Dowd A, Cortie MB (2009) The aluminium-copper-gold ternary system. Gold Bull 42:201–208
12. Bhatia VK, Kealley CS, Wuhrer R, Wallwork KS, Cortie MB (2009) Ternary β and γ phases in the Al-Au-Cu system at 750 °C. J Alloy Compd 488:100–107
13. Levey FC, Cortie MB, Cornish LA (2003) Determination of the 76 wt.% Au section of the Al-Au-Cu phase diagram. J Alloy Compd 354:171–180
14. Kodentsov AA, Bastin GF, Van Loo FJJ (2001) The diffusion couple technique in phase diagram determination. J Alloy Compd 320:207–217